

Effect of Organic and Inorganic Passivation in Quantum-Dot-Sensitized Solar Cells

Mauricio Solis de la Fuente,[†] Rafael S. Sánchez,[‡] Victoria González-Pedro,[‡] Pablo P. Boix,[§] S. G. Mhaisalkar,[§] Marina E. Rincón,[†] Juan Bisquert,[‡] and Iván Mora-Seró^{*,‡}

[†]Instituto de Energías Renovables, Universidad Nacional Autónoma de México, Apartado Postal 34, Temixco, Mor., México 62580

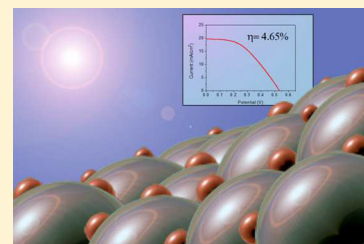
[‡]Photovoltaic and Optoelectronic Devices Group, Departament de Física, Universitat Jaume I, 12071 Castelló, Spain

[§]Energy Research Institute @ NTU (ERI@N), Nanyang Technological University, Research Techno Plaza, RTP/XF-05 50 Nanyang Drive, Singapore 637553

S Supporting Information

ABSTRACT: The effect of semiconductor passivation on quantum-dot-sensitized solar cells (QDSCs) has been systematically characterized for CdS and CdS/ZnS. We have found that passivation strongly depends on the passivation agent, obtaining an enhancement of the solar cell efficiency for compounds containing amine and thiol groups and, in contrast, a decrease in performance for passivating agents with acid groups. Passivation can induce a change in the position of TiO₂ conduction band and also in the recombination rate and nature, reflected in a change in the β parameter. Especially interesting is the finding that β , and consequently the fill factor can be increased with the passivation treatment. Applying this strategy, record cells of 4.65% efficiency for PbS-based QDSCs have been produced.

SECTION: Energy Conversion and Storage; Energy and Charge Transport



In the past few years, the interest in the use of light-absorbing inorganic semiconductor materials for nanostructured photovoltaic devices has increased enormously, in particular, in the case of semiconductor quantum dots (QDs), when the semiconductor particle size is smaller than its Bohr radius and quantum confinement regime is attained.^{1–7} These materials are extremely interesting for the development of photovoltaic applications for several reasons: tunable band gap, high extinction coefficient, large intrinsic dipole moment, and easy and cheap production.^{1–7} In fact, QD solar cells are announced as the next big thing in photovoltaics due to the huge potentiality of these materials in several different configurations.⁸ Among these configurations, quantum-dot-sensitized solar cells (QDSCs), where QDs act as light harvesters, have awakened a special interest. QDSCs benefit from the huge knowledge already achieved with dye-sensitized solar cells (DSCs) and from the easy preparation of this type of devices.

Despite its potentiality, the efficiency obtained for QDSCs has been significantly inferior to the record efficiency reported for DSCs (~12%).⁹ Currently, the maximum efficiency reported for CdS/CdSe light-absorbing material, the most extended semiconductors analyzed in QDSCs, is ~5.4%,^{10,11} and up to 6.3% has been obtained with Sb₂S₃.¹² Very recently we have reported an efficiency of 4.2% for PbS/CdS/ZnS based devices (unpublished results). Nevertheless, recent reports of solar cell efficiencies exceeding 10% for all solid nanostructured devices using lead halide perovskite have boosted the interest in semiconductor nanostructured light harvesters.^{13,14} The exact working principles of these perovskite solar cells are not well

understood, and some differences with conventional sensitized solar cells have been manifested in these devices.¹³ Moreover, these working principles have been studied for conventional QDSCs.^{15,16} In the present work, we have used this last configuration, QDSCs, to study the effect of QD passivation in the final cell performance.

Passivation of QDs has helped to increase significantly the efficiency of a third kind of solar cells using, in this case, a thin layer of colloidal QDs. In this last configuration, the QD colloidal layer is responsible for both light harvesting and charge transport. Organic^{17–19} and inorganic^{19,20} passivation have improved the solar cell performance of a thin layer of colloidal QDs solar cells, attaining efficiencies as high as 7% when hybrid passivation (organic and inorganic) is used.¹⁹ In the case of QDSC configuration, it is well known that the performance is improved significantly when the surface of QDs is coated with ZnS as an inorganic passivating agent.^{21–23} Moreover, several works in the literature report the functionalization of nanocrystals and metallic clusters by using a series of different organic species, including thiols,^{17,18,24,25} amines,²⁶ and carboxylic acids.²⁷ These molecules can passivate the surface states of QDs,¹⁹ introduce electrical dipoles,²⁴ and act as electron²⁰ or hole traps.²⁵

Our work, here reported, is focused on the effect in the performance of QDSC subjected to organic and inorganic

Received: March 21, 2013

Accepted: April 12, 2013

passivation. For that purpose, we have analyzed CdS, CdS/ZnS, and PbS/CdS/ZnS QDSCs, choosing dimethylamine (DMA), ethylenediamine (ETDA), ethanedithiol (EDT), thioglycolic acid (TGA), and formic acid (FA) as organic passivating agents and the halides in hexadecyl trimethylammonium chloride (HTAC) and tetrabutylammonium iodide (TBAI) as the inorganic passivating ligands (Figure 1). We have observed

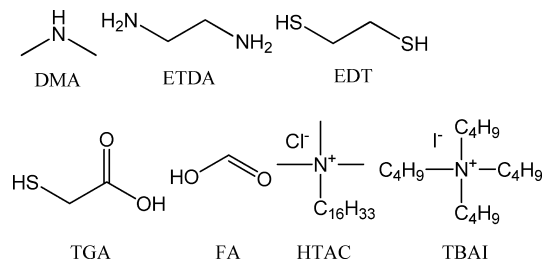


Figure 1. Chemical structure of the surface passivation agents employed.

that in many cases the passivation produces a beneficial effect in cell performance, especially due to an improvement in fill factor (FF). We found that the increase in FF is produced by an increase of β , an empirical parameter related to the electron recombination rate, U_n . In sensitized solar cells, β is the exponent of the electron density, n :²⁸

$$U_n = k_r n^\beta \quad (1)$$

where k_r is a constant. We have used this passivation strategy to push the efficiency of PbS/CdS QDSCs up to a value as high as 4.65%, as far as we know the highest efficiency for this material and configuration.

To analyze the fundamental effect of organic and inorganic passivation, we prepared CdS-sensitized electrodes. For comparison, the same passivation performed on CdS-sensitized electrodes was also carried out on CdS/ZnS-sensitized electrodes. It is already known that ZnS coating significantly enhances the efficiency of QDSCs due to an efficient passivation.^{21–23} The objective of passivated CdS/ZnS-sensitized electrodes was to verify if the good passivation performed by ZnS coating could be improved. Sample preparation and characterization methods are described in detail in the Supporting Information S11. In brief, nanostructured TiO₂ electrodes were sensitized by successive ionic layer adsorption and reaction (SILAR) method and sub-

sequently treated with the different organic ligands and inorganic precursors mentioned above. These molecules attach preferentially on the deposited semiconductor, instead of TiO₂, as SILAR deposition method practically covers all of the TiO₂ surface.¹⁵ Then, these electrodes were assembled with copper sulfide counter electrodes and aqueous polysulfide electrolyte to prepare the corresponding devices and study their performance. At least two electrodes were prepared under the same conditions of sensitizer and passivation agent, but more than two cells have been prepared in the case of reference cells and cells with the highest efficiencies.

The average current–potential (J – V) characteristics of these solar cells under simulated solar illumination (AM1.5, 100 mW·cm⁻²) are shown in Figure 2. The solar cell parameters corresponding to these J – V curves are summarized in Table 1.

Table 1. Averaged Cell Parameters for CdS and CdS/ZnS QD-Sensitized Cells, Plotted in Figure 2

	V_{oc} (V)	J_{sc} (mA/cm ²)	FF (%)	η (%)
CdS	0.460	7.39	43.1	1.45
DMA	0.503	8.56	52.5	2.36
ETDA	0.484	7.93	51.2	1.97
EDT	0.469	6.71	51.8	1.66
TGA	0.458	6.04	53.9	1.49
FA	0.348	3.53	48.4	0.61
HTAC	0.471	8.03	47.8	1.82
TBAI	0.386	5.98	43.2	1.00
CdS/ZnS	0.500	9.10	49.6	2.23
DMA	0.513	9.59	49.8	2.34
ETDA	0.508	9.53	53.2	2.64
EDT	0.520	8.91	52.9	2.50
TGA	0.490	7.59	53.6	1.99
FA	0.498	7.75	50.2	1.97
HTAC	0.542	7.07	47.5	1.95
TBAI	0.534	9.77	49.9	2.68

Cells based on CdS and CdS/ZnS samples without any additional passivation treatment were taken as standard reference devices. Table 1 indicates that ZnS passivation significantly increases the overall efficiency of CdS QDSCs from 1.45 to 2.23%, as it has been previously observed.^{21–23}

Comparing CdS and CdS/ZnS electrodes, Figure 2a,b respectively, broader dispersion of J – V curves with the different treatments is observed for CdS samples. Despite this dispersion, some general trends can be unveiled with the help

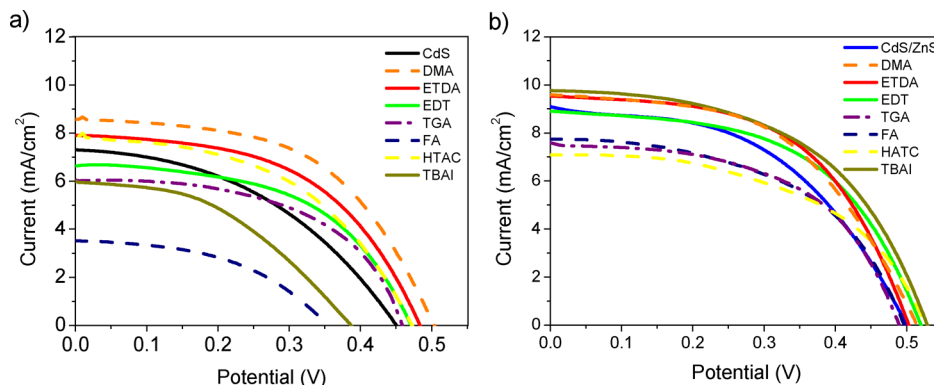


Figure 2. J – V curves of the (a) CdS and (b) CdS/ZnS QDSCs treated with different organic and inorganic surface passivation agents, obtained from averaging the J – V curves of the cells prepared under the same conditions.

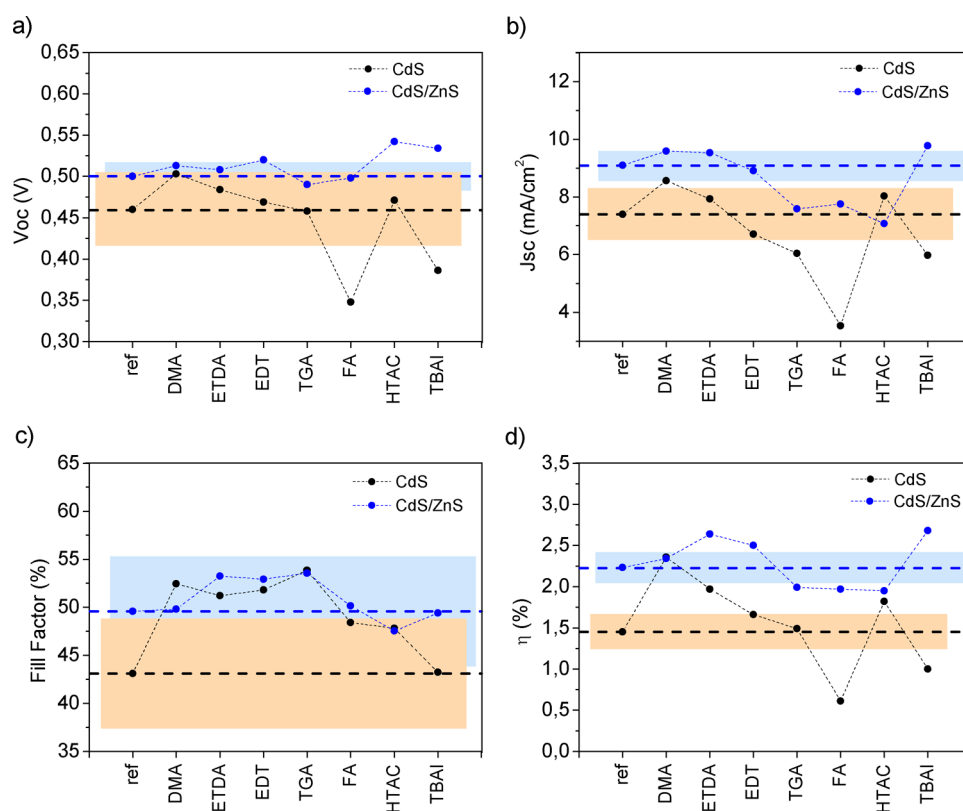


Figure 3. Cell parameter analysis of the CdS and CdS/ZnS QDSCs treated with different surface passivation agents. The shaded areas show the standard deviation (σ) for each cell parameter of the reference CdS, pink, and CdS/ZnS, blue, QDSCs, whereas black and blue dashed lines indicate the average value obtained for reference samples. Dotted lines are only eye guides and they cannot be considered as trend lines.

of Figure 3: (i) ZnS coating enhances the short circuit current, J_{sc} , open circuit potential, V_{oc} , FF, and consequently the conversion efficiency, η (see dashed lines in Figure 3). (ii) The effect of the other passivating agents is less significant than the effect of ZnS, but the appropriated ones can enhance the cell efficiency even for cells already passivated with ZnS. (iii) Alkylamines (DMA and ETDA) and alkylthiols (EDT) promote a clear increase in the cell efficiency in comparison to the reference devices, whereas the additives bearing carboxylic groups (TGA and FA) reduce cell performance for both CdS and CdS/ZnS electrodes. (iv) For inorganic passivation, the results depend on the semiconductor surface: CdS efficiency increases with Cl^- and decreases with I^- , while CdS/ZnS shows the opposite behavior. (v) Especially significant is the increase in FF that cannot be explained merely by the increase of V_{oc} observed in certain samples.²⁹

In view of the results obtained, we have analyzed our devices by impedance spectroscopy (IS) to find out a feasible explanation for the trends observed in the solar cell parameters after organic and inorganic passivation. Figure 4 shows the recombination resistance, R_{rec} , and chemical capacitance, C_{μ} , extracted from the IS measurements under dark conditions. For samples sensitized with CdS, these parameters are shown in Figure 4a,b, whereas for CdS/ZnS, R_{rec} and C_{μ} are shown in Figure 4c,d, respectively. Both R_{rec} and C_{μ} are represented as a function of $V_F = V_{app} - V_{series}$, which is the applied voltage, V_{app} , corrected by the voltage drop due to series resistance V_{series} .^{15,29} As it is observed in Figure 2, Figure 4 shows a higher dispersion of the results for CdS samples than for CdS/ZnS solar cells.

Comparing R_{rec} and C_{μ} for passivated and reference cells, it is possible to unravel the origin in the variation of V_{oc} .^{15,29} The

higher V_{oc} observed after passivation, in some cases, can be due to: (i) an upward shift of the conduction band (CB) of TiO_2 or (ii) a decrease in the recombination rate. Considering the first effect, an upward shift of the TiO_2 CB, it produces a solidarity movement of the TiO_2 electron quasi-Fermi level, which determines the cell V_{oc} and consequently an increase in open circuit potential. This displacement of the TiO_2 CB can be identified by a shift to higher potentials of C_{μ} (i.e., a horizontal shift of capacitance in Figure 4b,d). Moreover, the reduction of recombination rate can also be identified with IS by an increase in R_{rec} . This recombination process corresponds to the recombination of electrons in TiO_2 , which can recombine with the acceptor states in either the electrolyte or in the semiconductor light absorber.^{16,21}

Taking into account these considerations, some of the variations in the solar cell performance after passivation can be explained. For example, in the case of CdS QDSC passivated with DMA, an upward shift of TiO_2 CB is observed in Figure 4b. In addition, Figure 4a shows a higher R_{rec} than the reference cell at higher V_F potentials. Both effects point in the direction of V_{oc} enhancement as it is in fact observed. Passivation with ETDA also shows a higher R_{rec} than the reference cell but no significant shift of TiO_2 CB, giving a lower enhancement in V_{oc} than in the case of DMA. Note also that the different behavior observed for the inorganic passivation HTAC and TBAl for CdS and CdS/ZnS cells can be explained from the recombination resistances obtained after passivation. CdS electrodes passivated with Cl^- present higher R_{rec} and overall cell efficiency than CdS electrodes passivated with I^- ; see Figure 4a. However, the relative values of R_{rec} for HTAC and TBAl passivation are opposite for CdS/ZnS QDSCs;

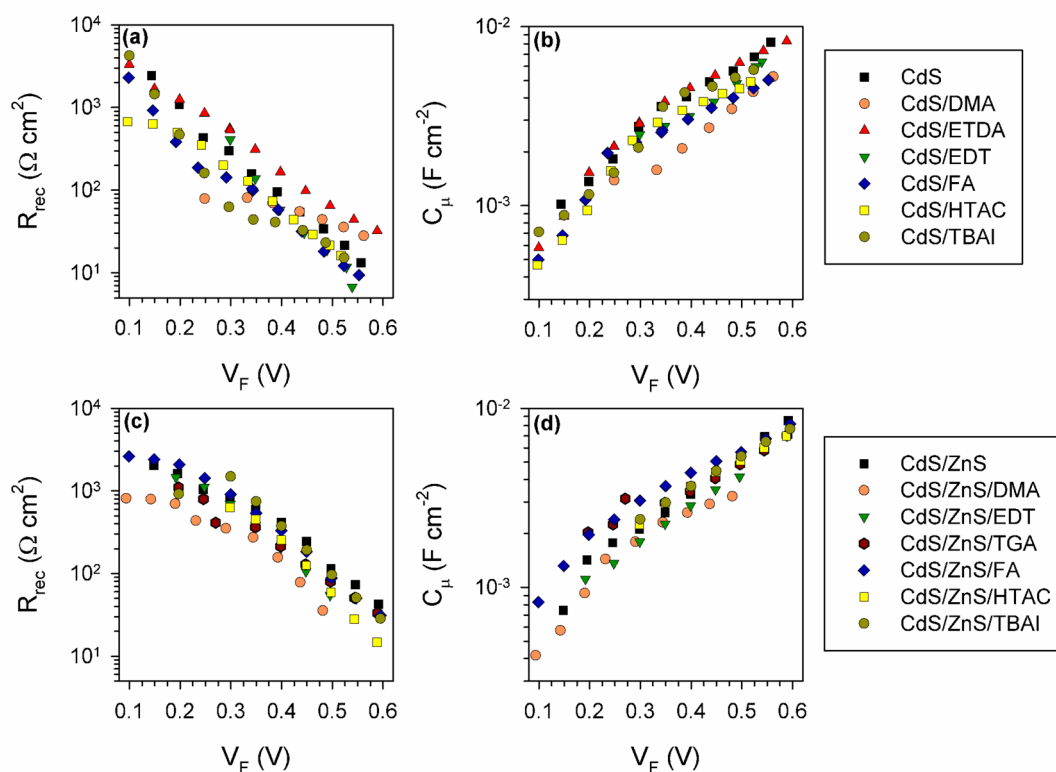


Figure 4. Recombination resistance, R_{rec} , extracted from the IS measurements under dark conditions for samples sensitized with (a) CdS and (c) CdS/ZnS; and chemical capacitance, C_{μ} , for (a) CdS and (c) CdS/ZnS QDSCs. To calculate V_F , we corrected the applied DC voltage by subtracting the voltage drop due to the total series resistance.

consequently, the best performance is obtained for I^- passivation in this case. The passivation reported in this work consists on a chemical surface treatment that can induce a shift of the TiO_2 CB or a change in the recombination properties of electrons in TiO_2 , the recombination process that can be scrutinized by IS, as it has been observed previously with molecular dipole treatments.²⁴

Concerning the variation in photocurrent, the different electrodes show similar light absorbance; see SI2 in the Supporting Information. This fact indicates that in most of the cases the changes observed in J_{sc} cannot be attributed to a variation in the light absorption properties after the passivation treatment. In these cases, a reduction in recombination rate produces an increase in V_{oc} as it has been already discussed, which also increases J_{sc} due to a shift of the J - V curve, and the reverse effect when recombination is augmented.

Treatments with alkylamines (DMA and ETDA) and alkylthiols (EDT) enhance the cell efficiency over the experimental error (see Figure 3d), even for CdS/ZnS cells. Despite the contrasted goodness of ZnS coating to improve the efficiency of QDSCs,^{21–23} it is not a perfect passivating agent, and it leaves more room for further QDSC performance improvement. Passivation with carboxylic groups (TGA and FA) did not significantly improve, or even worsen, the performance of the cells. The differences observed among alkylamine- (DMA and ETDA) and alkylthiol- (EDT) treated cells and TGA and FA could be ascribed to the relatively low $\text{p}K_a$ of the carboxylic groups ($\text{p}K_{a\text{FA}} = 3.77$ ³⁰ and $\text{p}K_{a\text{TGA}} = 3.67$ ³¹). This low $\text{p}K_a$ could induce the QD corrosion or

deactivation and its subsequent partial loss of functionality; see SI2 in the Supporting Information.

Moreover, it is well known that amines can enhance the luminescence of semiconductor particles by reducing the nonradiative recombination.^{26,32} An increase of the photoluminescence was also observed for CdSe-sensitized electrodes after ZnS coating.²¹ Passivation of surface states reduces internal recombination in the QD (before injection and nonaccessible by IS experiments), thus enhancing the photo-injection and consequently the final photocurrent. In this sense, injection efficiency for QDSCs could be close to one, as it is considered for the most common dyes in DSCs,³³ only with an appropriate passivation.

Finally and concerning the evolution of cell parameters after passivation, a significant enhancement of FF is detected in most of the analyzed cases; see Figure 3c. The increase of the FF values is especially significant for cells without ZnS coating, but even for CdS/ZnS electrodes further improvement can be attained after passivation. Variation of FF can be due to two reasons: (i) a change in the series resistance or (ii) a change in the β parameter, defined in eq 1.^{28,29} No significant change in the series resistance of passivated QDSCs was observed, as it has been analyzed by IS measurements of R_{series} ; see SI3 in the Supporting Information. Therefore, we suggest that the increase of the FF is ascribed to an increase of the β values after passivation, as in fact is the general trend observed in Figure 5. β has been obtained from several samples and the average values are plotted in Figure 5. β is calculated from the slope of Figure 4a,c graphs as:^{28,29}

$$R_{rec} = R_0 \exp(-\beta q V_F / k_b T) \quad (1)$$

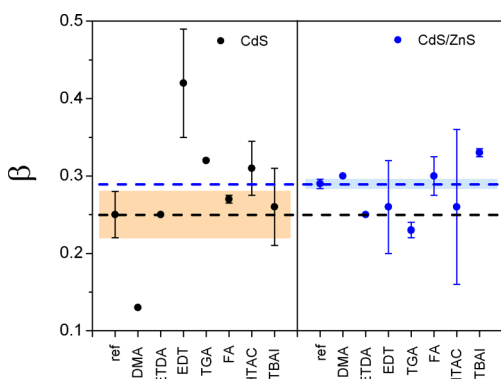


Figure 5. Average value of β parameter, eq 1, from the slope of $\ln(R_{\text{rec}})$ versus V_F (Figure 4a,c), obtained from CdS and CdS/ZnS reference QDSCs and for the cells with different passivations.

where R_0 is a preexponential factor, q is the electron charge, k_b is the Boltzmann constant, and T is the temperature. Passivation produces a change in the recombination process that affects the β parameter, enhancing its value and consequently FF. The description of the exact physical mechanisms producing this change is below the scope of this work, and it will require a model for the β parameter in QDSCs that has not been developed yet.

Once we observed that the best results were obtained with CdS/ZnS-based devices and being conscious of the importance of the surface passivation on the efficiency of the cells, the chemical treatment was applied before and after coating the CdS with the ZnS layer; this means a double passivation treatment. In this case, only the treatments with an alkylamine, an alkylthiol, and the inorganic iodide were tested, since these treatments yielded the best performance of the devices with a single passivation; see Table 1. Figure 6 and Table 2 show the

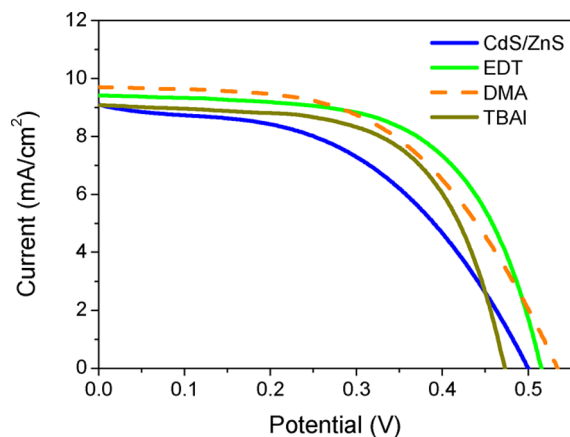


Figure 6. J - V curves of devices with double surface passivation based on CdS/ZnS light absorber.

Table 2. Cell Parameters for Double Surface Passivation of CdS/ZnS-Based Devices

	V_{oc} (V)	J_{sc} (mA/cm ²)	FF (%)	η (%)
CdS/ZnS	0.500	9.08	49.6	2.23
EDT	0.515	9.60	60.1	2.97
DMA	0.534	9.78	52.9	2.76
TBAI	0.472	9.07	62.2	2.67

J - V curves and the cell parameters of the devices prepared with the double passivation methodology, and in all cases, the performance of the devices was improved compared with the reference device CdS/ZnS. Moreover, FF values were higher after the corresponding treatments, especially in the cases of EDT and TBAI with more than 20% enhancement (see Table 2), which is in agreement with the results previously obtained. It is worth highlighting that after the double treatment with EDT a record efficiency device ($\eta \approx 3\%$) based on CdS/ZnS light absorber was obtained, which means a 105% enhancement of the efficiency compared to the reference device based on CdS (and a significant 33% enhancement with respect to the CdS/ZnS reference). This is, as far as we know, one of the highest efficiencies reported for QDSCs using only CdS as light-absorbing material.

CdS is an excellent material for the analysis and optimization of different treatments and procedures for QDSCs due to its easy and relatively fast preparation by SILAR at room temperature and air atmosphere, but the final efficiency is limited by its band gap that confines the visible light absorption to the shorter wavelengths, consequently limiting J_{sc} ; see SI4 in the Supporting Information. In contrast, PbS is a narrow band-gap semiconductor that allows us to extend the light absorption to the near-infrared region;^{34–36} see SI4 in the Supporting Information. Taking advantage of the light-absorbing properties of PbS nanocrystals and the use of our surface passivation methodology, we aimed for the development of high-performance QDSC based on PbS/CdS/ZnS semiconductors. CdS/ZnS coating of PbS decreases recombination and significantly enhances the cell stability with polysulfide electrolyte.³⁴ Figure 7 and Table 3 show the averaged and record cell results

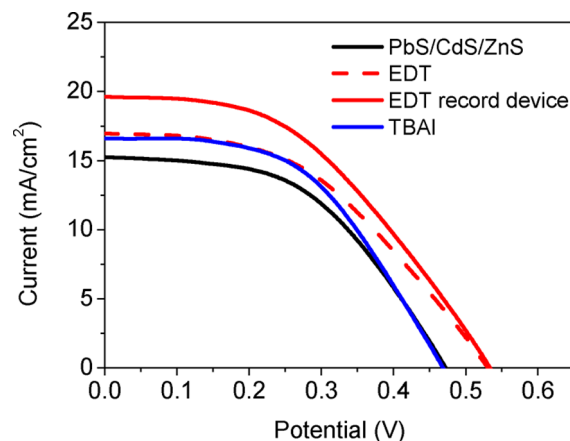


Figure 7. J - V curves of devices with double surface passivation based on PbS/CdS/ZnS as light absorber.

obtained for PbS/CdS/ZnS-based devices, where the double-passivation treatment (after CdS and after ZnS deposition, no

Table 3. Cell Parameters for the Double Surface Passivation of PbS/CdS/ZnS-Based Devices

	V_{oc} (V)	J_{sc} (mA/cm ²)	FF (%)	η (%)
PbS/CdS/ZnS	0.471	15.37	49.8	3.57
EDT ^a	0.532	19.64	44.5	4.65
EDT ^b	0.529	16.98	45.6	4.09
TBAI	0.468	16.63	50.7	3.94

^aRecord efficiency device values. ^bAverage values of different devices.

passivation was performed on PbS surface) was applied using EDT and TBAL. As in the previous analyzed cases, the passivation treatments enhance the final solar cell performance, obtaining a record cell with $\eta = 4.67\%$, 11% higher than our previous results with no passivation treatment (unpublished results). As far as we know, this is the highest efficiency reported for a PbS-based QDSC. Note that in this case no significant enhancement of FF is observed due to the high increase in photocurrent that produces a higher voltage drop at the series resistance.

In summary, the effect of surface passivation in QDSCs with organic and inorganic compounds has been analyzed. In the case of organic passivation, alkylamines (DMA and ETDA) and the alkylthiol (EDT) treatments improved the cell performance, while additives bearing carboxylic groups (TGA and FA) did not contribute significantly or even worsen it. In the case of the inorganic passivation with I and Cl, it could also improve cell performance, but in this case it is important on which material the treatment is performed, and different results are obtained for I and Cl depending on the material (CdS or ZnS) in which the treatment is carried out. The origin of the observed differences in cell parameters has been explained by IS characterization. The boost of the FF values after passivation, which arises from an increase of the β parameter, is especially interesting. This observation is particularly remarkable for QDSCs, where low β are observed.^{15,34,37} For QDSCs, the reported FFs are still not comparable with DSCs regardless of a significant reduction on the series resistance obtained with the use of alternative counter electrodes.¹⁵ This work shows an efficient strategy to improve β value and consequently FF. This strategy has been used to improve conversion efficiency in CdS/ZnS and PbS/CdS/ZnS QDSCs, obtaining values as high as 2.97 and 4.65%, respectively, the highest reported for these systems up to our knowledge.

■ ASSOCIATED CONTENT

● Supporting Information

Materials and methods, light absorption measurements, series resistance, and IPCE for CdS, CdS/ZnS, and PbS/CdS/ZnS. This material is available free of charge via the Internet at <http://pubs.acs.org>.

■ AUTHOR INFORMATION

Corresponding Author

*E-mail: sero@uji.es.

Notes

The authors declare no competing financial interest.

■ ACKNOWLEDGMENTS

This work was supported by the Institute of Nanotechnologies for Clean Energies (INCE), funded by the Generalitat Valenciana under Project ISIC/2012/008. We thank the following agencies for support of this research: Ministerio de Educacion y Ciencia under project HOPE CSD2007-00007, Generalitat Valenciana (ISIC/2012/008), and Universitat Jaume I project 12I361.01/1. We acknowledge projects CYTED-Nanoenergía, PAPIIT-IN106912 (UNAM-México), and CONACyT-153270 (México) for financial support. M.S.F. acknowledges the fellowship given by CONACyT-México. Funding from National Research Foundation (NRF) Singapore is also kindly acknowledged (CRP Award No. NRF-CRP4-2008-03).

■ REFERENCES

- (1) Hodes, G. Comparison of Dye- and Semiconductor-Sensitized Porous Nanocrystalline Liquid Junction Solar Cells. *J. Phys. Chem. C* **2008**, *112*, 17778–17787.
- (2) Kamat, P. V.; Tvrdy, K.; Baker, D. R.; Radich, J. G. Beyond Photovoltaics: Semiconductor Nanoarchitectures for Liquid-Junction Solar Cells. *Chem. Rev.* **2010**, *110*, 6664–6688.
- (3) Mora-Seró, I.; Bisquert, J. Breakthroughs in the Development of Semiconductor-Sensitized Solar Cells. *J. Phys. Chem. Lett.* **2010**, *1*, 3046–3052.
- (4) Rühle, S.; Shalom, M.; Zaban, A. Quantum-Dot-Sensitized Solar Cells. *Chem. Phys. Chem.* **2010**, *11*, 2290–2304.
- (5) Hetsch, F.; Xu, X.; Wang, H.; Kershaw, S. V.; Rogach, A. L. Semiconductor Nanocrystal Quantum Dots as Solar Cell Components and Photosensitizers: Material, Charge Transfer, and Separation Aspects of Some Device Topologies. *J. Chem. Phys. Lett.* **2011**, *2*, 1879–1887.
- (6) Yang, Z.; Chen, C.-Y.; Roy, P.; Chang, H.-T. Quantum Dot-Sensitized Solar Cells Incorporating Nanomaterials. *Chem. Commun.* **2011**, *47*, 9561–9571.
- (7) Alivisatos, A. P. Semiconductor Clusters, Nanocrystals, and Quantum Dots. *Science* **1996**, *271*, 933–937.
- (8) Kamat, P. V. Quantum Dot Solar Cells. The Next Big Thing in Photovoltaics. *J. Phys. Chem. Lett.* **2013**, *4*, 908–918.
- (9) Yella, A.; Lee, H.-W.; Tsao, H. N.; Yi, C.; Chandiran, A. K.; Nazeeruddin, M. K.; Diao, E. W.-G.; Yeh, C.-Y.; Zakeeruddin, S. M.; Grätzel, M. Porphyrin-Sensitized Solar Cells with Cobalt (II/III)-Based Redox Electrolyte Exceed 12% Efficiency. *Science* **2011**, *334*, 629–634.
- (10) Santra, P. K.; Kamat, P. V. Mn-Doped Quantum Dot Sensitized Solar Cells: A Strategy to Boost Efficiency over 5%. *J. Am. Chem. Soc.* **2012**, *134*, 2508–2511.
- (11) Pan, Z.; Zhang, H.; Cheng, K.; Hou, Y.; Hua, J.; Zhong, X. Highly Efficient Inverted Type-I CdS/CdSe Core/Shell Structure QD-Sensitized Solar Cells. *ACS Nano* **2012**, *6*, 3982–3991.
- (12) Chang, J. A.; Im, S. H.; Lee, Y. H.; Kim, H.-j.; Lim, C.-S.; Heo, J. H.; Seok, S. I. Panchromatic Photon-Harvesting by Hole-Conducting Materials in Inorganic–Organic Heterojunction Sensitized-Solar Cell through the Formation of Nanostructured Electron Channels. *Nano Lett.* **2012**, *12*, 1863–1867.
- (13) Lee, M. M.; Teuscher, J.; Miyasaka, T.; Murakami, T. N.; Snaith, H. J. Efficient Hybrid Solar Cells Based on Meso-Superstructured Organometal Halide Perovskites. *Science* **2012**, *338*, 643–647.
- (14) Kim, H.-S.; Lee, C.-R.; Im, J.-H.; Lee, K.-B.; Moehl, T.; Marchioro, A.; Moon, S.-J.; Humphry-Baker, R.; Yum, J.-H.; Moser, J. E.; Grätzel, M.; Park, N.-G. Lead Iodide Perovskite Sensitized All-Solid-State Submicron Thin Film Mesoscopic Solar Cell with Efficiency Exceeding 9%. *Sci. Rep.* **2012**, *2*, 591.
- (15) González-Pedro, V.; Xu, X.; Mora-Seró, I.; Bisquert, J. Modeling High-Efficiency Quantum Dot Sensitized Solar Cells. *ACS Nano* **2010**, *4*, 5783–5790.
- (16) Hod, I.; González-Pedro, V.; Tachan, Z.; Fabregat-Santiago, F.; Mora-Seró, I.; Bisquert, J.; Zaban, A. Dye versus Quantum Dots in Sensitized Solar Cells: Participation of Quantum Dot Absorber in the Recombination Process. *J. Chem. Phys. Lett.* **2011**, *2*, 3032–3035.
- (17) Barkhouse, D. A. R.; Pattantyus-Abraham, A. G.; Levina, L.; Sargent, E. H. Thiols Passivate Recombination Centers in Colloidal Quantum Dots Leading to Enhanced Photovoltaic Device Efficiency. *ACS Nano* **2008**, *2*, 2356–2362.
- (18) Zhao, N.; Osedach, T. P.; Chang, L.-Y.; Geyer, S. M.; Wanger, D.; Binda, M. T.; Arango, A. C.; Bawendi, M. G.; Bulovic, V. Colloidal PbS Quantum Dot Solar Cells with High Fill Factor. *ACS Nano* **2010**, *4*, 3743–3752.
- (19) Ip, A. H.; Thon, S. M.; Hoogland, S.; Voznyy, O.; Zhitomirsky, D.; Debnath, R.; Levina, L.; Rollny, L. R.; Carey, G. H.; Fischer, A.; et al. Hybrid Passivated Colloidal Quantum Dot Solids. *Nat. Nanotechnol.* **2012**, *7*, 577–582.
- (20) Tang, J.; Kemp, K. W.; Hoogland, S.; Jeong, K. S.; Liu, H.; Levina, L.; Furukawa, M.; Wang, X.; Debnath, R.; Cha, D.; et al.

Colloidal-Quantum-Dot Photovoltaics Using Atomic-Ligand Passivation. *Nat. Mater.* **2011**, *10*, 765–771.

(21) Guijarro, N.; Campiña, J. M.; Shen, Q.; Toyoda, T.; Lana-Villarreal, T.; Gómez, R. Uncovering the Role of the ZnS Treatment in the Performance of Quantum Dot Sensitized Solar Cells. *Phys. Chem. Chem. Phys.* **2011**, *13*, 12024–12032.

(22) Shen, Q.; Kobayashi, J.; Diguna, L. J.; Toyoda, T. Effect of ZnS Coating on the Photovoltaic Properties of CdSe Quantum Dot-Sensitized Solar Cells. *J. Appl. Phys.* **2008**, *103*, 084304.

(23) Mora-Seró, I.; Giménez, S.; Fabregat-Santiago, F.; Gómez, R.; Shen, Q.; Toyoda, T.; Bisquert, J. Recombination in Quantum Dot Sensitized Solar Cells. *Acc. Chem. Res.* **2009**, *42*, 1848–1857.

(24) Barea, E. M.; Shalom, M.; Giménez, S.; Hod, I.; Mora-Seró, I.; Zaban, A.; Bisquert, J. Design of Injection and Recombination in Quantum Dot Sensitized Solar Cells. *J. Am. Chem. Soc.* **2010**, *132*, 6834–6839.

(25) Guijarro, N.; Lana-Villarreal, T.; Lutz, T.; Haque, S. A.; Gómez, R. Sensitization of TiO₂ with PbSe Quantum Dots by SILAR: How Mercaptophenol Improves Charge Separation. *The J. Phys. Chem. Lett.* **2012**, *3*, 3367–3372.

(26) Bullen, C.; Mulvaney, P. The Effects of Chemisorption on the Luminescence of CdSe Quantum Dots. *Langmuir* **2006**, *22*, 3007–3013.

(27) Zamborini, F. P.; Hicks, J. F.; Murray, R. W. Quantized Double Layer Charging of Nanoparticle Films Assembled Using Carboxylate/(Cu²⁺ or Zn²⁺)/Carboxylate Bridges. *J. Am. Chem. Soc.* **2000**, *122*, 4514–4515.

(28) Bisquert, J.; Mora-Seró, I. Simulation of Steady-State Characteristics of Dye-Sensitized Solar Cells and the Interpretation of the Diffusion Length. *J. Phys. Chem. Lett.* **2010**, *1*, 450–456.

(29) Fabregat-Santiago, F.; Garcia-Belmonte, G.; Mora-Seró, I.; Bisquert, J. Characterization of Nanostructured Hybrid and Organic Solar Cells by Impedance Spectroscopy. *Phys. Chem. Chem. Phys.* **2011**, *13*, 9083–9118.

(30) Braude, E. A.; Nachod, F. C. *Determination of Organic Structures by Physical Methods*; Academic Press: New York, 1955.

(31) Edsall, J. T.; Wyman, J. *Biophysical Chemistry*; Academic Press: New York, 1958.

(32) Dannhauser, T.; O'Neil, M.; Johansson, K.; Whitten, D.; McLendon, G. Photophysics of Quantized Colloidal Semiconductors. Dramatic Luminescence Enhancement by Binding of Simple Amines. *J. Phys. Chem.* **1986**, *90*, 6074–6076.

(33) Nazeeruddin, M. K.; Kay, A.; Rodicio, I.; Humphry-Baker, R.; Mueller, E.; Liska, P.; Vlachopoulos, N.; Graetzel, M. Conversion of light to electricity by *cis*-X₂Bis(2,2'-bipyridyl-4,4'-dicarboxylate)-ruthenium(II) Charge-Transfer Sensitizers (X = Cl⁻, Br⁻, I⁻, CN⁻, and SCN⁻) on Nanocrystalline Titanium Dioxide Electrodes. *J. Am. Chem. Soc.* **1993**, *115*, 6382–6390.

(34) Braga, A.; Giménez, S.; Concina, L.; Vomiero, A.; Mora-Seró, I. Panchromatic Sensitized Solar Cells Based on Metal Sulfide Quantum Dots Grown Directly on Nanostructured TiO₂ Electrodes. *J. Phys. Chem. Lett.* **2011**, *2*, 454–460.

(35) Hossain, M. A.; Koh, Z. Y.; Wang, Q. PbS/CdS-Sensitized Mesoscopic SnO₂ Solar Cells for Enhanced Infrared Light Harnessing. *Phys. Chem. Chem. Phys.* **2012**, *14*, 7367–7374.

(36) Zhou, N.; Chen, G.; Zhang, X.; Cheng, L.; Luo, Y.; Li, D.; Meng, Q. Highly Efficient PbS/CdS Co-Sensitized Solar Cells Based on Photoanodes with Hierarchical Pore Distribution. *Electrochem. Commun.* **2012**, *20*, 97–100.

(37) Hossain, M. A.; Jennings, J. R.; Shen, C.; Pan, J. H.; Koh, Z. Y.; Mathews, N.; Wang, Q. CdSe-Sensitized Mesoscopic TiO₂ Solar Cells Exhibiting >5% Efficiency: Redundancy of CdS Buffer Layer. *J. Mater. Chem.* **2012**, *22*, 16235–16242.